ACS APPLIED MATERIALS & INTERFACES

Letter

www.acsami.org

Understanding the Electrochemical Mechanism of K-αMnO$_2$ for Magnesium Battery Cathodes

Timothy S. Arthur,*[,†] Ruigang Zhang,[†] Chen Ling,[†] Per-Anders Glans,[‡] Xudong Fan,[§] Jinghua Guo,[‡] and Fuminori Mizuno[†]

[†]Toyota Research Institute of North America, 1555 Woodridge Avenue, Ann Arbor, Michigan 48105, United States

[‡]Advanced Light Source, Lawrence Berkeley National Laboratory, 1 Cyclotron Road, Berkeley, California 94720, United States

[§]Center for Advanced Microscopy, Michigan State University, East Lansing, Michigan 48824, United States

Supporting Information

ABSTRACT: Batteries based on magnesium are an interesting alternative to current state-of-the-art lithium-ion systems; however, high-energy-density cathodes are needed for further development. Here we utilize TEM, EDS, and EELS in addition to soft-XAS to determine electrochemical magnesiation mechanism of a high-energy density cathode, K-αMnO$_2$. Rather than following the typical insertion mechanism similar to Li$^+$, we propose the gradual reduction of K-αMnO$_2$ to form Mn$_2$O$_3$ then MnO at the interface of the cathode and electrolyte, finally resulting in the formation of K-αMnO$_2$@(Mg,Mn)O core−shell product after discharge of the battery. Understanding the mechanism is a vital guide for future magnesium battery cathodes.

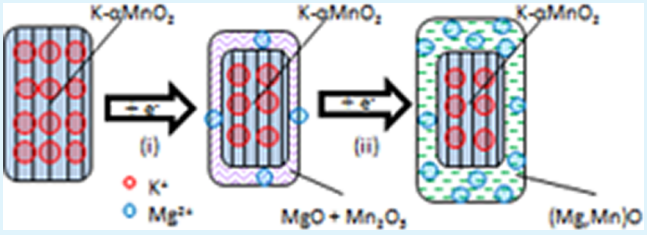

KEYWORDS: *magnesium batteries, cathodes, transmission electron microscopy, soft-X-ray absorption spectroscopy*

The emergence of hybrid, plug-in hybrid, and electric vehicles has had a significant role in reducing green-house gas emissions. However, diversification of electrochemical energy storage is vital to improving the range, cost, and safety of electric vehicles.[1] Batteries based on a multivalent Mg^{2+} ion are an interesting alternative to current Li$^+$ ion technology. Compared to lithium metal, the magnesium metal anode provides a higher volumetric energy density, 2061 mAh cm^{-3} (Li) to 3833 mAh cm^{-3} (Mg), greater natural abundance, and potential safety advantages due to nondendritic electrochemical deposition.[2,3] Recently, research has focused on synthesizing electrolytes capable of magnesium metal deposition/dissolution and wide oxidation stability.[4,5] Alternatively, researchers have also proposed insertion anodes coupled with magnesium trifluoromethanesulfonyl imide electrolytes as a route to reach high voltage magnesium-ion batteries.[6−8] However, to realize multivalent Mg-based energy storage systems, new cathode materials capable of intercalating Mg^{2+} ions need to be developed. The prototypical intercalation cathode for magnesium batteries is a Chevrel phase molybdenum sulfide (Mo_3S_4) cathode. However, the low reduction potential (~1.1 V vs Mg) and reversible capacity (120 mAh g^{-1}) inhibit high energy-density battery systems.

Decades of research has been dedicated to discovering intercalation cathodes for magnesium batteries.[9] Gregory et al. reported the successful chemical and electrochemical insertion of Mg^{2+} into various transition metal oxides and sulfides, and Novak et al.[10] describe effective intercalation is accomplished through screening of the Mg^{2+} ion with water molecules. Recently, incremental increases to energy density have been shown by two-dimensional cathodes,[11] polyanion cathodes,[12] and thin-film sputtered cathodes.[13] Previously, we proposed a Hollandite phase, potassium-stabilized manganese dioxide (K-αMnO$_2$) as a candidate cathode material for Mg batteries.[14] On the initial discharge, the system showed 282 mAh g^{-1} specific capacity, however, the capacity quickly faded to 134 mAh g^{-1} on the second cycle and continues to fade with cycling (see Figure S1a,b in the Supporting Information). When used as a Li-ion battery cathode, K-αMnO$_2$ retains 75% of the initial capacity,[15] as compared to 52% for Mg batteries. The discrepancy prompted our investigations into the magnesiation mechanism for K-αMnO$_2$ for Mg batteries. Our initial analysis of the cathode using X-ray photoelectron spectroscopy (XPS), and hard X-ray absorption spectroscopy revealed that although the electrochemical magnesiation effectively reduced Mn^{4+}, complete reoxidation could not be accomplished within the electrolyte stability window (~3.2 V vs Mg). Furthermore, the appearance of new Bragg diffractions or peak-shift was not detected via X-ray diffraction (XRD), however, a decrease in peak intensity for K-αMnO$_2$ after magnesiation was observed. The challenge is to determine if the cathode follows the same intercalation path as in Li$^+$ ion systems, because such knowledge will guide future synthetic strategies. Here, we use transmission electron microscopy (TEM) analysis techniques

Received: March 13, 2014
Accepted: May 7, 2014
Published: May 7, 2014

dx.doi.org/10.1021/am5015327 | ACS Appl. Mater. Interfaces 2014, 6, 7004−7008

and soft X-ray absorption spectroscopy (soft-XAS) to determine the mechanism for the first discharge of a Mg/K-αMnO_2 battery.

TEM is an extremely powerful technique to observe the nanoscale crystallographic or morphologic changes in cathode which affect the bulk electrochemical properties.[16−18] To avoid reactions with oxygen and moisture, all TEM samples were analyzed without exposure to air. Figure 1a−d shows TEM

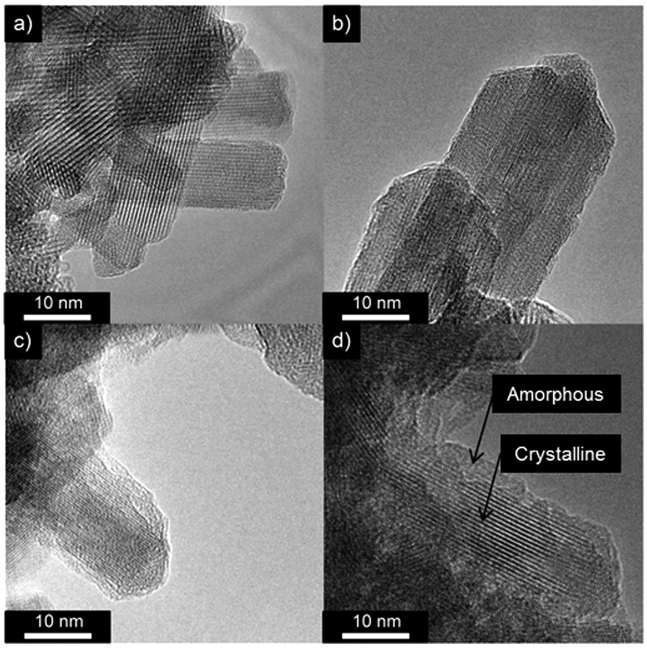

Figure 1. TEM images of the cathode at the (a) Pristine, (b) 33 DOD, (c) 66 DOD, and (d) 100 DOD states of the first discharge.

micrographs of a K-αMnO_2 cathode at different of depths-of-discharge (DOD): Pristine (0 mAh g^{-1}, 0 Mg/Mn), 33 DOD (93 mAh g^{-1}, ~0.16 Mg/Mn), 66 DOD (187 mAh g^{-1}, ~0.32 Mg/Mn), and 100 DOD (280 mAh g^{-1}, ~0.47 Mg/Mn), respectively. A significant morphological change in the cathode nanoparticles was apparent during electrochemical magnesiation. The pristine nanoparticles are approximately 20 nm (l) × 10 nm (d) crystalline nanorods where the lattice fringes clearly extend to the edges of the individual nanorods. Upon electrochemical reduction to 66 DOD, a noncrystalline layer appears on the surface, whereas crystalline grains are still observed in the center of the nanorod. The formation of the core@shell morphology is not caused chemically by soaking the cathode in the electrolyte (see TEM micrographs in Figure S2 in the Supporting Information), and therefore is electrochemically induced upon reduction of the cathode in the electrolyte. In addition, the amorphous material was always connected to a crystalline core, and thus the formation of the product did not remove the shell from the core. Similar to our previous XRD results, new crystalline phases could not be detected in the selected area electron diffraction pattern of the completely discharged cathode. In comparison, TEM investigation of K-αMnO_2 after the first electrochemical lithiation shows the crystalline lattices extending to the edges of the nanorods (see Figure S3 in the Supporting Information). The formation of the inorganic, amorphous layer is unique consequence of the first electrochemical magnesiation.

Discovery of the core@shell morphology encouraged a deeper analysis of the core and shell components after discharge. Scanning-tunneling electron microscopy (STEM) and energy dispersive X-ray spectroscopy (EDS) microanalysis of a 100 DOD nanorod is shown in Figure 2 (top). To improve

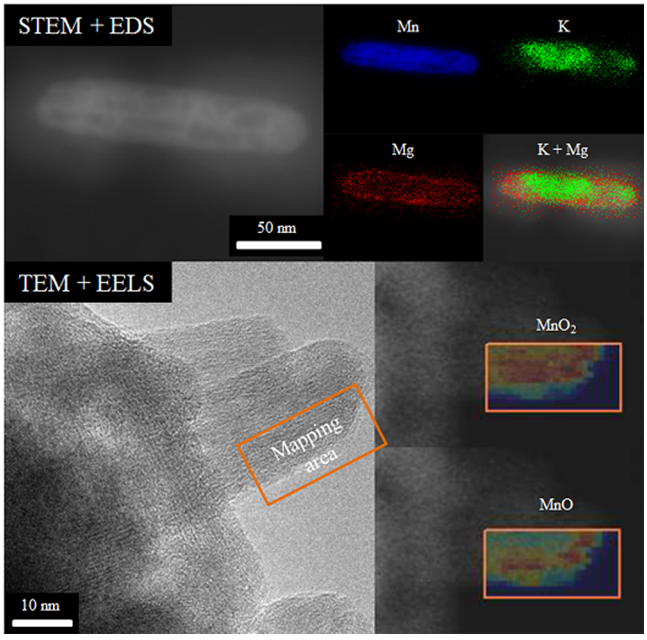

Figure 2. Scanning tunneling electron microscope (STEM) image with EDS mapping (top) and TEM with EELS mapping (bottom) of K-αMnO_2 at 100 DOD.

the spatial resolution, 120 nm (l) × 40 nm (d) nanorods of K-αMnO_2 were mapped to determine the elemental dispersion throughout the cathode. Figure S1c,d in the Supporting Information shows that although the larger nanorods have a lower initial discharge capacity of 117 mAh g^{-1}, they also suffer from severe first-cycle capacity fade. The majority of the magnesium is located in the shell of the discharged cathode (noncrystalline), whereas the potassium is located primarily in the core (crystalline). The lack of potassium from the shell of the cathode after discharge could arise from (i) dissolution of the K^+ into the organohaloaluminate electrolyte, (ii) displacement of K^+ with Mg^{2+} during electrochemical reduction, or (iii) diffusion of K^+ into the core of the cathode during electrochemical reduction. Although EDS illustrates a uniform dispersion of Mn throughout the discharged cathode, we were encouraged to use electron energy-loss spectroscopy (EELS) of the Mn *M*-edge cathode to determine the changes oxidation state of Mn throughout the discharged cathode (Figure 2 - bottom). The total spectrum can be deconvoluted into two manganese components; Mn^{4+} (referenced by MnO_2) and Mn^{2+} (referenced by MnO). Figure 2 clearly shows the higher concentrations of Mn^{2+} in the shell and Mn^{4+} in the core. From the EDS mapping, we have distinguished a clear potassium and magnesium separation in the core and shell, respectively. From the EELS mapping, manganese is reduced to Mn^{2+} in the shell, whereas Mn^{4+} remains in the core. The evidence implies that the core remains unreacted K-αMnO_2, whereas the reduction of manganese proceeds on the shell of the nanorod. Interestingly, the loss of potassium in the shell implies that K^+ is either expelled into the electrolyte or diffuses into the core of the

dx.doi.org/10.1021/am5015327 | ACS Appl. Mater. Interfaces 2014, 6, 7004−7008

electrode. From this result, we are encouraged to investigate the role of the stabilizing cation concentration and size for αMnO_2.

To further substantiate our claim that the two electron reduction of manganese occurs only on the surface of the cathode, we also performed soft-XAS measurements, inspired by researchers that have illustrated how in-depth analysis of the Fe *L*-edge was key to decipher the electronic structure of lithium iron-phosphate during electrochemical cycling.[19] For this work, the Mn *L*-edge provides element specific evidence for the unoccupied d-orbitals key to identifying specific oxidation states, and is surface sensitive when the absorbance is detected through total electron yield. Figure 3a shows the spectra of the

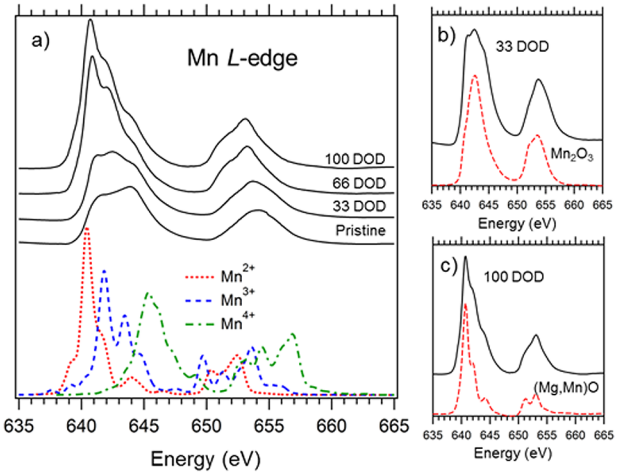

Figure 3. (a) Mn *L*-edge soft-XAS of K-αMnO_2 electrochemically magnesiated to different depths-of-discharge (DOD). Calculated spectra of Mn^{2+}, Mn^{3+}, and Mn^{4+} (symmetry = O_h, crystal-field splitting = 1.0 eV) are shown below. (b) Mn *L*-edge comparison of 33 DOD to Mn_2O_3 and (c) 100 DOD to (Mg,Mn)O.

Pristine, 33 DOD, 66 DOD, and 100 DOD cathodes. In addition, we calculated the spectra for Mn^{2+}, Mn^{3+} and Mn^{4+} using the program CTM4XAS[20] by keeping the crystal field splitting =1.0 eV and symmetry = O_h unchanged and varying the oxidation state. We feel confident in this methodology because from our previous extended X-ray absorption fine structure work on the Mn *K*-edge,[14] we determined that the MnO_6 octahedra were maintained during magnesiation, but an increase in local disorder after magnesiation was shown by a loss in signal intensity and the disappearance of the Mn−Mn_{corner} sharing peak. Therefore, the symmetry of the Mn remains O_h and intact throughout electrochemical reduction, however, deviations in the crystal field splitting of the products are possible. The calculation highlights a clear difference between the position and intensity of the Mn *L*-edge due to manganese oxidation state, a unique advantage of soft X-ray analysis. The Mn L_3-edge of the Pristine cathode is composed of two peaks at 644 and 641 eV indicating Mn^{4+} and Mn^{3+} (from potassium stabilization), respectively. At 33 DOD, the appearance of a signal at 642 eV indicates the presence of an additional manganese species which finger-prints well to powdered Mn_2O_3 (Figure 3b). A sharp peak appearing at 640 eV shows that formation of Mn^{2+} upon magnesiation of K-αMnO_2 from 0.16 to 0.32 Mg/Mn. After complete discharge, the spectrum shows a small shift of the Mn L_3-edge to lower energies and an increase of the Mn^{2+} peak. In Figure 3c, the completely reduced cathode was compared to a MgO:MnO (1:1) solid-solution synthesized through planetary ball-milling, and although not amorphous to XRD (see Figure S3 in the Supporting Information), the spectrum is very similar to that of the 100 DOD cathode. Direct finger-printing of MnO was not possible due to experimental limitations, as noticed by previous researchers.[21] However, the soft-XAS results validate the observation of Mn^{2+} seen in the shell with TEM analysis and identifies key species during electrochemical reduction. With a confident understanding of the reaction products, we can propose a mechanism for the electrochemical magnesiation of the cathode.

Our initial discharge capacity for a Li^+ ion system is 252 mAh g^{-1} at an average voltage of 2.5 V vs Li. The similarity of the initial magnesiation capacity, the voltage profile and our previous analysis pointed to the same electrochemical pathway between Mg^{2+} and Li^+. However, the theoretical capacity, considering a $2e^-$ reduction of Mn^{4+} to Mn^{2+}, of K-αMnO_2 is ~600 mAh g^{-1} depending on the concentration of potassium used to stabilize the structure. The initial specific discharge capacity of 280 mAh g^{-1} can easily be interpreted by a single electron reduction of the entire cathode $Mn^{4+} \rightarrow Mn^{3+}$, which is the preferred Li^+ ion pathway.[15] However, a two electron reduction of half the cathode $Mn^{4+} \rightarrow 0.5\ Mn^{2+} + 0.5\ Mn^{4+}$ would show the same capacity, and dissuades us from relying purely on Coulombic charge measurements to determine the mechanism. From our extensive analysis, we propose that Mg^{2+} ion does not mimic Li^+ ion insertion into K-αMnO_2 during discharge, but rather undergoes different electrochemical and chemical reactions

$$0.5Mg^{2+} + 2MnO_2 + e^- \rightarrow Mg_{0.5}MnO_2 + MnO_2 \quad (1)$$

$$Mg_{0.5}MnO_2 \rightarrow 0.5MgO + 0.5Mn_2O_3 \quad (2)$$

$$0.5Mn_2O_3 + 0.5Mg^{2+} + e^- \rightarrow (Mg_{0.5}Mn)O_{1.5} \quad (3)$$

$$Mg^{2+} + 2MnO_2 + 2e^- \rightarrow (Mg, Mn)O(shell) + MnO_2(core) \quad (4)$$

We propose the reaction proceeds through an initial insertion of Mg^{2+} (1) into the α-MnO_2 cathode. However, because of the thermodynamic instability of the $Mg_{0.5}MnO_2$, a phase transition reaction (2) occurs to form an amorphous mixture of MgO and Mn_2O_3. An alternate interpretation of our results is the direct formation of the amorphous mixture of Mn_2O_3/MgO through a conversion reaction. Without *in operando* diffraction techniques, capturing $Mg_{0.5}MnO_2$ is difficult because the final product is an amorphous mixture of MgO and Mn_2O_3. Previous researchers have shown electrochemical transformation of the hollandite structure to a more thermodynamically stable state for αMnO_2 in aqueous systems.[22] As the electrochemical magnesiation and reduction proceeds, Mn_2O_3 in the MgO/Mn_2O_3 mixture is reduced to an amorphous (Mg,Mn)O phase only on the shell of the cathode (3). Therefore, the final reaction (4) product is the transformation of K-αMnO_2 to K-αMnO_2@(Mg,Mn)O, rather than the intercalated $Mg_{0.5}MnO_2$. A detailed study of the Mg^{2+} kinetics coupled with *in operando* analysis would decipher between the direct conversion and intercalation/phase transition possibilities. The recognition of a different mechanism from the typical Li^+ ion insertion is the first step to developing a better magnesium cathode.

Although praised as high capacity alternatives to intercalation chemistry, conversion cathodes suffer from high polarization

between the discharge and charging voltage, loss of electronic contact caused by pulverization, as well as low Coulombic efficiency due to irreversibility of the electrochemical reactions.[23] Specifically for K-αMnO$_2$, we propose the formation of a mixture of two wide band gap insulators, MgO and MnO. From the deep investigation of the products, the phase transformation during magnesiation is the major cause of the capacity fading for K-αMnO$_2$ as a magnesium battery cathode. Figure 4a) is the soft-XAS Mn *L*-edge spectra

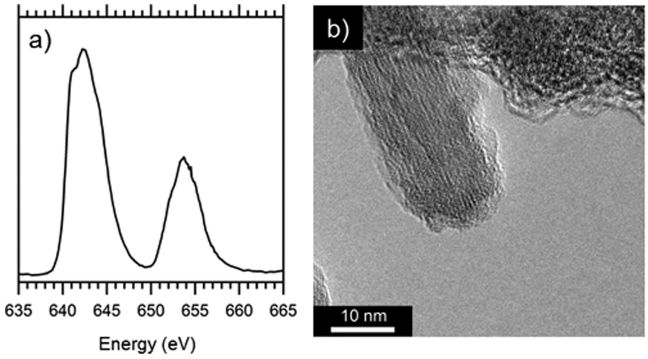

Figure 4. (a) Mn *L*-edge soft-XAS and (b) TEM image of K-αMnO$_2$ charged to 3.0 V vs Mg.

of the cathode electrochemically reoxidized to 3.0 V vs Mg. We observe a reduction in the Mn^{2+} intensity, however, complete reversibility of the cathode is not observed as the Mn^{3+} peak of the MgO/Mn_2O_3 mixture is still observed. Additionally, the TEM image in Figure 4b) shows the amorphous shell remaining on the surface of the nanorod after reoxidation. Regeneration of the crystalline K-αMnO$_2$ is not possible, and raising the voltage of our system to more positive limits risks electrolyte decomposition.[24] Importantly, we have chosen multiple avenues to pursue from the mechanistic understanding of the electrochemical magnesiation. First, we can continue to search for different oxide polymorphs where intercalation is the preferred magnesiation pathway,[25] rather than focusing on the hollandite phase. Second, improvement to the initial discharge capacity can be achieved through decreasing the dimensions of the K-αMnO$_2$ cathode to utilize more of the core. Finally motivated from the reversible Mn^{2+} oxidation in the shell, we can design amorphous solids as cathodes for reversible for Mg batteries. For example, NaMnO$_2$I and V_2O_5–P_2O_5 cathodes[26,27] are potential synthetic targets and can be revisited in hopes of improving Mg battery cathodes.

In conclusion, through a combination of microscopic and spectroscopic techniques, we have identified key steps in the electrochemical magnesiation of K-αMnO$_2$. As opposed to the typical intercalation mechanism observed in Li-ion batteries, a conversion reaction is the proposed mechanism. Our results suggest that the search for magnesium cathodes requires in-depth analysis without the presumption that lithium and magnesium follow the same path. Deciphering the true electrochemical mechanisms of electrodes is vital to finding the next high-energy-density Mg battery.

■ ASSOCIATED CONTENT

Supporting Information

Discharge curves for small and large K-αMnO$_2$. TEM images of soaked nanorods and electrochemically lithiated K-αMnO$_2$. XRD pattern of ball-milled 0.5MgO–0.5MnO powders. Additional Experimental Details. This material is available free of charge via the Internet at http://pubs.acs.org.

■ AUTHOR INFORMATION

Corresponding Author

*E-mail: tim.arthur@tema.toyota.com. Tel: 734-995-0674. Fax: 734-995-2549.

Author Contributions

The manuscript was written through contributions of all authors. All authors have given approval to the final version of the manuscript.

Notes

The authors declare no competing financial interest.

■ ACKNOWLEDGMENTS

The authors thank Dr. Masaki Matsui for important discussions about K-αMnO$_2$. The work at the Advanced Light Source is supported by the Director, Office of Science, Office of Basic Energy Science, of the U.S, Department of Energy, under Contract DE-AC02-05CH11231.

■ REFERENCES

(1) Armand, M.; Tarascon, J.-M. Building Better Batteries. *Nature* **2008**, *451*, 652–657.

(2) Aurbach, D.; Lu, Z.; Schechter, A.; Gofer, Y.; Gizbar, H.; Turgeman, R.; Cohen, Y.; Moshkovich, M.; Levi, E. Prototype Systems for Rechargeable Magnesium Batteries. *Nature* **2000**, *407*, 724–727.

(3) Gregory, T. D.; Hoffman, R. J.; Winterton, R. C. Non-aqueous Electrochemistry of Magnesium. *J. Electrochem. Soc.* **1990**, *137*, 775–780.

(4) Yoo, H. D.; Shterenberg, I.; Gofer, Y.; Gershinsky, G.; Pour, N.; Aurbach, D. Mg Rechargeable Batteries: An On-going Challenge. *Energy Environ. Sci.* **2013**, *6*, 2265–2279.

(5) Muldoon, J.; Buccur, C. B.; Oliver, A. G.; Sugimoto, T.; Matusi, M.; Kim, H. S.; Allred, G. D.; Zajicek, J.; Kotani, Y. Electrolyte Roadblocks to a Magnesium Rechargeable Battery. *Energy Environ. Sci.* **2012**, *5*, 5941–5950.

(6) Arthur, T. S.; Singh, N.; Matsui, M. Electrodeposited Bi, Sb and $Bi_{1-x}S_x$ Alloys as Anodes for Mg-ion Batteries. *Electrochem. Commun.* **2012**, *16*, 103–106.

(7) Singh, N.; Arthur, T. S.; Ling, C.; Matsui, M.; Mizuno, F. A High-energy Density Tin Anode for Rechargeable Magnesium ion Batteries. *Chem. Commun.* **2013**, *49*, 149–151.

(8) Shao, Y.; Gu, M.; Li, X.; Nie, Z.; Zuo, P.; Li, G.; Liu, T.; Xiao, J.; Cheng, Y.; Wang, C.; Zhang, J.-G.; Liu, J. Highly Reversible Mg Insertion in Nanostructured Bi for Mg ion Batteries. *Nano Lett.* **2014**, *14*, 255–260.

(9) Levi, E.; Gofer, Y.; Aurbach, D. On the Way to Rechargeable Mg Batteries: the Challenge of Cathode Materials. *Chem. Mater.* **2010**, *22*, 860–868.

(10) Novák, P.; Imhof, R.; Haas, O. Magnesium Insertion Electrodes for Rechargeable Nonaqueous Batteries – a Competitive Alternative to Lithium? *Electrochim. Acta* **1999**, *45*, 351–367.

(11) Liu, Y.; Lifang, J.; Wu, Q.; Du, J.; Zhao, Y.; Si, Y.; Wang, Y.; Yuan, H. Sandwich-structured Grapheme-like MoS_2/C Microspheres for Rechargeable Mg Batteries. *J. Mater. Chem. A* **2013**, *1*, 5822–5826.

(12) NuLi, Y.; Yang, J.; Wang, J.; Li, Y. Electrochemical Intercalation of Mg^{2+} in Magnesium Manganese Silicate and its Application as High-energy Rechargeable Magnesium Battery Cathode. *J. Phys. Chem. C* **2009**, *113*, 12594–12597.

(13) Gershinsky, G.; Yoo, H. D.; Gofer, Y.; Aurbach, D. Electrochemical and Spectroscopic Analysis of Mg^{2+} Intercalation into Thin Film Electrodes of Layered Oxides: V_2O_5 and MoO_3. *Langmuir* **2013**, *29*, 10964–10972.

(14) Zhang, R.; Yu, X.; Nam, K.-W.; Ling, C.; Arthur, T. S.; Song, W.; Knapp, A. M.; Ehrlich, S. N.; Yang, X.-Q.; Matsui, M. α-MnO_2 as a

Cathode for Rechargeable Mg Batteries. *Electrochem. Commun.* **2012**, *23*, 110−113.
(15) Thackery, M. M. Manganese Oxides for Lithium Batteries. *Prog. Solid State Chem.* **1997**, *25*, 1−71.
(16) Kawamoto, N.; Tang, D.-M.; Wei, X.; Wang, X.; Mitome, M.; Brando, Y.; Golberg, D. Transmission Electron Microscope as an Ultimate Tool for Nanomaterial Property Studies. *Microscopy* **2013**, *62*, 157−175.
(17) Liu, X. H.; Liu, Y.; Kushima, A.; Zhang, S.; Zhu, T.; Li, J.; Huang, J. Y. In Situ TEM Experiments of Electrochemical Lithiation and Delithiation of Individual Nanostructures. *Adv. Energy Mater.* **2012**, *2*, 722−741.
(18) Wang, F.; Robert, R.; Chernova, N. A.; Pereira, N.; Omenya, F.; Badway, F.; Hua, X.; Ruotolo, M.; Zhang, R.; Wu, L.; Volkov, V.; Su, D.; Key, B.; Whittingham, M. S.; Grey, C. P.; Amatucci, G. G.; Zhu, Y.; Greatz, J. Conversion Reaction Mechanisms in Lithium ion Batteries: Study of the Binary Metal Fluoride Electrodes. *J. Am. Chem. Soc.* **2011**, *133*, 18828−18836.
(19) Liu, X.; Liu, J.; Qiao, R.; Yu, Y.; Li, H.; Suo, L.; Hu, Y.-S.; Chuang, Y.-D.; Shu, G.; Chou, F.; Weng, T.-C.; Nordlund, D.; Sokoras, D.; Wang, Y. J.; Song, H. L.; Liu, Z.; Yan, S.; Liu, G.; Qiao, S.; Richardson, T. J.; Pendergast, D.; Hussain, Z.; de Groot, F. M. F.; Yang, W. Phase Transformations and Lithiation Effect on Electronic Structure of Li_xFePO_4: An In-depth Study by Soft X-ray and Simulations. *J. Am. Chem. Soc.* **2012**, *134*, 13708−13715.
(20) Stavitski, E.; de Groot, F. M. F. The CTM4XAS Program for EELS and XAS Spectral Shape and Analysis of Transition Metal *L*-edges. *Micron* **2010**, *41*, 687−694.
(21) Gilbert, B.; Frazer, B. H.; Belz, A.; Conrad, P. G.; Nealson, K. H.; Haskel, D.; Lang, J. C.; Srajer, G.; De Stasio, G. Multiple Scattering Calculations of Bonding and X-ray Absorption Spectroscopy of Manganese Oxides. *J. Phys. Chem. A* **2003**, *107*, 2839−2847.
(22) Larcher, D.; Courjai, P.; Urbina, R. H.; Gerand, B.; Blyr, A.; Du Pasquier, A.; Tarascon, J.-M. Synthesis of MnO_2 Phases from $LiMn_2O_4$ in Aqueous Media: Mechanisms of Phase Transformations, Reactivity, and Effect of Bi Species. *J. Electrochem. Soc.* **1998**, *145*, 3392−3400.
(23) Cabana, J.; Moncoduit, L.; Larcher, D.; Palacin, M.-R. Beyond Intercalation-based Li-ion Batteries: the State-of-the-Art and Challenges of Electrode Materials Acting Through Conversion Reactions. *Adv. Mater.* **2010**, *22*, E170−E192.
(24) Kim, H. S.; Arthur, T. S.; Allred, G. D.; Zajicek, J.; Newman, J. G.; Rodnyansky, A. E.; Oliver, A. G.; Boggess, W. C.; Muldoon, J. Structure and Compatibility of a Magnesium Electrolyte with a Sulphur Cathode. *Nat. Commun.* **2011**, *1435*, 1−6.
(25) Ling, C.; Mizuno, F. Phase-stability of Post-spinel Compound AMn_2O_4 (A = Li, Na, or Mg) and its Application as a Rechargeable Battery Cathode. *Chem. Mater.* **2013**, *25*, 3062−3071.
(26) Kim, J.; Manthiram, A. A Manganese Oxyiodide Cathode for Rechargeable Lithium Batteries. *Nature* **1997**, *390*, 265−267.
(27) Sakurai, Y.; Yamaki, J. Correlation Between Microstructure and Electrochemical Behaviour of Amorphous V_2O_5-P_2O_5 in Lithium Cells. *J. Electrochem. Soc.* **1988**, *135*, 791−796.